High-field Mössbauer study of manganese-zinc ferrites

A. H. Morrish
Department of Physics, Monash University, Clayton, Victoria, Australia 3168 and University of Manitoba, Winnipeg, Manitoba, Canada R3T 2N2

P. E. Clark
Department of Physics, Monash University, Clayton, Victoria, Australia 3168

(Received 29 July 1974)

The disordered ferrite system, $Mn_{1-x}Zn_xFe_2O_4$ for $0 \leq x \leq 0.95$ has been studied by the Mössbauer-effect technique at 4.2 K in applied magnetic fields of 50 and 90 kOe. In these fields a ferrimagnetic structure is implied for the entire family of compounds. For $x = 0$ the cation distribution is $(Mn_{0.82}Fe_{0.18})[Mn_{0.18}Fe_{1.82}]O_4$; for larger x the iron concentration on A (tetrahedral) sites decreases, and becomes less than 2 at.% by $x = 0.6$. For $x \geq 0.6$, some of the Fe ions on B (octahedral) sites have their spin moments reversed. Within the experimental error, the magnetic moments of the iron ions are collinear for $x < 0.5$ and noncollinear for $x > 0.5$. The canting angles for normal B-site cations are found to increase with increasing zinc content, and to depend on the applied field. The sample with $x = 0.80$ has the most stable structure. The hyperfine fields and isomer shifts show only a small variation with sample composition.

I. INTRODUCTION

The properties of magnetically disordered ferrites have been a subject of considerable interest for over 20 years.[1-4] In particular, mixed systems containing zinc have received much attention, especially in the past five or six years.[5-11] The saturation magnetization of these systems at first increases linearly with zinc content, but then decreases when more than 50-at.% Zn is present.[1] Neutron-diffraction and Mössbauer spectroscopy experiments on Ni-Zn ferrites[5-8] have established that their magnetic structure is noncollinear in the zinc-rich region. Recently, by applying large magnetic fields up to 90 kOe, the Mössbauer spectra of Co-Zn[12] and Ni-Zn[13] ferrites have been more fully resolved; as a result the complex spin structures of these systems have been clarified. This paper reports on similar experiments for the Mn-Zn ferrite system.

One feature that makes an investigation of the Mn-Zn ferrites especially worthwhile is the difference in cation distributions. As is well known, the mixed zinc ferrites have the spinel structure, and the cations occupy one A (tetrahedral) and two B (octahedral) sites per formula unit. When the divalent ions are all located on A sites the structure is called a normal spinel, whereas when they are all on B sites the structure is called an inverse spinel. Between these two extremes, partial inversion of any amount is possible. There is mounting evidence that the diamagnetic Zn^{2+} ions occupy A sites only. Therefore it is useful to concentrate on the site occupancy of the magnetic divalent cations in the mixed zinc ferrites.

For $Ni_{1-x}Zn_xFe_2O_4$, all the magnetic divalent ions Ni^{2+} are situated at B sites for the entire range of x.[7,13] For $Co_{1-x}Zn_xFe_2O_4$, the Co^{2+} ions also prefer the B sites. For the end member ($x=0$), 75–90% of the cobalt ions, depending on the heat treatment, occupy B sites.[14] This percentage increases to close to 100% for $x \geq 0.4$.[12] Thus both these families of compounds are either fully or highly inverted with respect to the magnetic cations.

On the other hand, for $Mn_{1-x}Zn_xFe_2O_4$, the manganese ions show a preference for the A sites. For $x=0$, earlier neutron-diffraction and Mössbauer results gave the formula[14,15] $(Mn_{0.8}Fe_{0.2})[Mn_{0.2}Fe_{1.8}]O_4$, where the round and square brackets refer to ions occupying A and B sites, respectively. More recent neutron-diffraction data[16] gave $(Mn_{0.85}Fe_{0.15})[Mn_{0.15}Fe_{1.85}]O_4$ for $x=0$, $(Zn_{0.20}Mn_{0.72}Fe_{0.08})[Mn_{0.08}Fe_{1.92}]O_4$ for $x=0.2$, and, within the experimental error, no manganese ions on B sites for $x \geq 0.4$.

In the high-field work on Co-Zn and Ni-Zn ferrite,[12,13] there was evidence that at high Zn concentrations some iron ions on B sites had their magnetic moments reversed, that is, had moments with components parallel rather than antiparallel to the A-sublattice magnetization. However, the presence of iron cations on the A sites obscured the analysis. The absence of iron cations on A sites in the Zn-rich region of the Mn-Zn ferrites should provide less ambiguous data on this effect.

It is useful to summarize the recent literature on the Mn-Zn ferrites. Cser *et al.*[9] have collected Mössbauer spectra of $Mn_{1-x}Zn_xFe_2O_4$ for $0 \leq x$

≤ 0.80 from liquid-nitrogen temperature to above the ferrimagnetic Néel temperature in zero applied magnetic field. They have assumed that the Fe^{3+} ions occupy B sites only, and have fitted up to four overlapping six-line patterns to the broad absorption lines. The different patterns were related to the relative probabilities for various Mn-Zn ion configurations on the six nearest-neighbor A sites. The variation with temperature of the hyperfine fields associated with each pattern was determined. It was even suggested that Fe^{3+} ions with six Zn^{2+} nearest neighbors would have reversed moments.

For the compound $Mn_{0.6}Zn_{0.4}Fe_2O_4$, König *et al.*[10] have determined the magnetizations of the A and B sublattices between 20 and 600 K by neutron diffraction, as well as the hyperfine field at Fe^{57} nuclei on B sites between 80 and 350 K from Mössbauer spectra. From an analysis of these results they concluded that the molecular-field constant is zero for the A-A interaction, and, surprisingly, is positive for the B-B interaction.

Bashkirov *et al.*[11] have obtained Mössbauer spectra from liquid-nitrogen temperature to above the ferrimagnetic Néel point, with and without a magnetic field of 16 kOe applied perpendicular to the propagation direction of the γ ray. They find that 5–15% of the A sites are occupied by Fe^{3+} ions, and, although the corresponding value of x was not given, it would appear that the zinc concentration was low. For the one example discussed in detail ($x = 0.3$), the cation distribution was found to be $(Zn_{0.3}Mn_{0.6}Fe_{0.1})[Mn_{0.1}Fe_{1.9}]O_4$. A total of ten overlapping six-line patterns were fitted to the spectrum. The nine B-site patterns were ascribed to different configurations of the Zn, Mn, and Fe ions of the six nearest-neighbor A sites.

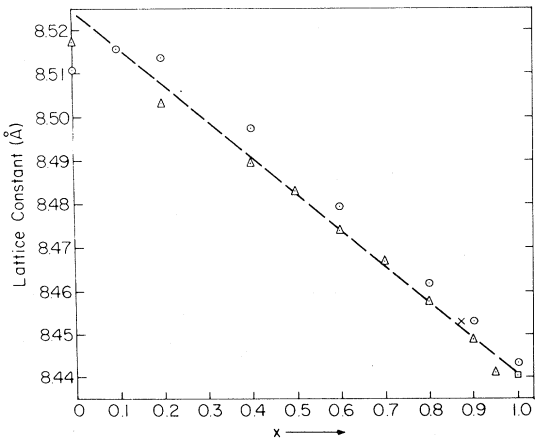

FIG. 1. Lattice constants as a function of zinc content for $Mn_{1-x}Zn_xFe_2O_4$. (○): data from König and Chol (Ref. 16); (X): data from Fayek *et al.* (Ref. 17); (□): data from Leung *et al.* (Ref. 7); (△): data from this work.

There have been several investigations of the magnetic structure at 4.2 K for $x > 0.8$ by neutron diffraction. Fayek *et al.*[17] conclude that $Mn_{0.13}Zn_{0.87}Fe_2O_4$ is antiferromagnetic, with an ordering temperature at about 11 K. For compounds with slightly less zinc ($0.82 \leq x \leq 0.87$), Loshmanov *et al.*[18] find that both ferrimagnetic and short-range antiferromagnetic order coexist at low temperatures. As x increases the degree of short-range antiferromagnetic order increases, becoming long range by $x = 0.87$. The ferrimagnetic Néel temperature for $x = 0.84$ is about 375 K. The neutron-diffraction pattern for the end member, $ZnFe_2O_4$, is similar to that for $x = 0.87$.[17,19,20] Several magnetic structures for the B sublattice are compatible with the experimental results, but a noncollinear model with four sublattices appears to be favored. The ordering arrangement on the A sublattice has not been determined.

II. EXPERIMENTAL

The $Mn_{1-x}Zn_xFe_2O_4$ series were prepared by dissolving stoichiometric amounts of the corresponding metals in dilute sulfuric acid. After dehydration at room temperature, stearic acid (2%) was added as a binder. The mixture was pressed into pellets and fired at 1300°C in an argon atmosphere. X-ray powder diffraction photographs were taken with Mn-filtered Fe $K\alpha$ radiation. The observed lines were well defined, and were all indexed in terms of a single-phase spinel structure. The lattice constants are plotted as a function of zinc content in Fig. 1, and compared with other values reported earlier. The data are approximately linear, except perhaps $x < 0.3$. The deviation, if any, is less than that found by König and Chol,[16] who, however, prepared their samples by ceramic techniques.

Mössbauer spectra were obtained at 4.2 K with a constant-acceleration transducer and a multichannel analyzer operating in the time mode. The samples were mounted at the center of a superconducting solenoid. The magnetic field was applied parallel to the direction of propagation of the Fe^{57} γ rays. The source was Co^{57} in Cu, and was inserted inside the cryostat. Although the fringing field at the source was 4% of the applied field, the screening effect in the copper host produced negligible splitting in the single-line emission. Spectra were collected in applied fields of 50 and 90 kOe as well as without a field. The spectra were calibrated with an absorber of thin iron foil. The sample absorbers were thin, and were made by dispersing the Mn-Zn ferrite powder in benzophenone.

III. RESULTS

The Mössbauer spectra were fitted with Lorentzian-shaped lines by the method of least squares with the aid of computers, both at Monash and Manitoba. The philosophy adopted was to employ the minimum number of distinct hyperfine fields necessary to obtain an acceptable value of the least-squares parameter, χ^2. Corresponding pairs of lines of the spectra were constrained to have the same intensity and linewidth. For some of the fits of the in-field spectra, electric quadrupole shifts were deduced. The values obtained were small (usually less than 0.04 mm/s), with an error of at least ± 100%. Therefore, within the experimental limitations, the electric quadrupole interaction may be taken to be zero to first order. This result is expected for a polycrystalline ferrimagnet in a sufficiently strong external magnetic field. The lack of resolution of the overlapping patterns for the zero-field spectra did not permit a meaningful determination of the quadrupole shifts to be made.

It was found possible to fit all the zero-field spectra with two six-line patterns. The in-field spectra, on the other hand, have been fitted employing three hyperfine fields. For $x < 0.5$, four-line patterns were used, whereas for $x > 0.5$, six-line patterns were necessary. An iron impurity in a beryllium disk, sometimes used in the sample holder, produced a small central peak in some of the spectra. This problem was overcome by making a suitable adjustment in the computer program. Typical in-field spectra are illustrated in Fig. 2; the solid curves are the sum of the three individual patterns used to fit the data.

IV. DISCUSSION

The zero-field Mössbauer spectra consisted of six absorption lines for all values of x. However, appreciable differences in intensity and linewidth in corresponding pairs of lines clearly show that a minimum of two six-line patterns is present. Respectable values of χ^2 were obtained with just two patterns. The two hyperfine fields differed by about 10 kOe (± 5) for all compositions. The largest hyperfine field was about 521 kOe for all x, except for the end member, $MnFe_2O_4$, for which it was about 513 kOe. The linewidth (full width at half-maximum intensity) of the same line for different zinc contents was sensibly constant (~0.5 mm/sec). However, the in-field spectra established that a minimum of three patterns were present. Therefore, further analysis of the system is based on the in-field spectra; the zero-field data serve merely as a consistency check.

It is convenient to develop the discussion under various subheadings based on the parameters that can be extracted from the in-field spectra.

A. Hyperfine fields

By inspection, the in-field spectra, illustrated in Fig. 2, consist of at least three patterns, one outermost pattern and, because corresponding pairs of lines are asymmetric, two inner patterns. The values of the three hyperfine fields deduced from the spectra obtained at 50 kOe are plotted as a function of zinc content in Fig. 3. The two fields that are decreased with an increase in the applied field are to be related to ferric ions that have a magnetic-moment component aligned parallel to the direction of this applied field, that is, ions that occupy B sites. These two groups of ions are denoted B_1 and B_2 (Fig. 3). Since the other hyperfine field is increased, it is to be associated with ions with a magnetic-moment component antiparallel to the applied field. For $MnFe_2O_4$, these ions occupy A sites. However, for larger zinc contents at least, there are no iron ions on A

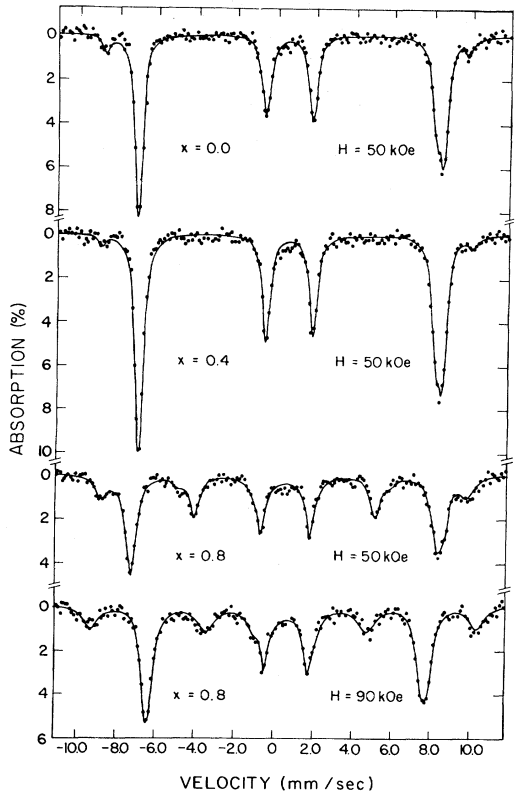

FIG. 2. Typical Mössbauer spectra of $Mn_{1-x}Zn_xFe_2O_4$ at 4.2 K in external applied magnetic fields of 50 or 90 kOe. The full curve is the sum of the three individual patterns required to fit the data.

sites according to the neutron diffraction results of König and Chol.[16] Hence, these ions are located on B sites, but have their moments reversed; this configuration will be denoted B_3. For some intermediate value of x, the origin of the outer absorption patterns will shift from ions on A sites to ions on B sites. A maximum in the larger hyperfine field occurs at $x \approx 0.5$, which suggests that that may be where the shift occurs. Of course, for the approximate range $0.4 < x < 0.6$, ions on both A and B sites may be contributing to the absorption, and this possibility is indicated by the dashed lines in Fig. 3. However, the absorption is too small and the counting rate insufficient to permit any structure in the absorption lines to be resolved. This tentative identification of the A and B_3 spectra will receive confirmation in Sec. IV B.

It is of interest to consider the hyperfine fields and their dependence on composition, especially in relation to the results obtained on other mixed spinel systems. For $MnFe_2O_4$, the magnitude of the hyperfine field at the A sites in zero applied field is less than that at the B sites. A similar result is observed for $NiFe_2O_4$ and $CoFe_2O_4$. However, for $MnFe_2O_4$, the difference is smaller, about 15 kOe, which explains why the third pattern was not resolved in the zero-field spectra. The smaller A-site field is believed to be primarily due to a larger covalency, and therefore to a greater degree of spin delocalization at the A sites. The u parameter has been reported[16] to be 0.3865, which implies that the Fe^{3+}-O^{2-} internuclear separation for the A sites is about 0.05 Å smaller than that for B sites. This difference of 0.05 Å is less than that of 0.11 Å for $NiFe_2O_4$, for example, and accounts for the smaller difference in the hyperfine fields at the two sites.

It is attractive to attempt to account for the variation in hyperfine fields with zinc content on the basis of the supertransferred hyperfine field H_{sthf}.[7,12] This field is essentially the covalent contribution to the total hyperfine field from spin transfer and overlap effects between neighboring magnetic ions. These covalent interactions may occur directly between the two cations, or indirectly via an intermediate oxygen anion. It is usual to assume the largest effects are between ions on A and B sites, viz., the next-nearest-neighbor cation d orbitals, the nearest-neighbor-ligand σ orbitals, and the $4s$ orbitals of the cation under consideration. The supertransferred hyperfine interaction between ions on A sites is believed to be small, primarily because the internuclear separation distance is large. On the other hand, the interaction between two ions on B sites is probably important, but is neglected because reliable theoretical calculations are lacking.

Generally, the hyperfine field at Fe^{57} on an A site shows little, if any, change with zinc content. For $(CoZn)Fe_2O_4$, the A-site field, for zero applied field, increases slightly from 500 to 515 kOe for $x = 0.0$–0.5, and then decreases to 505 kOe by $x = 0.8$. The initial increase is suggested to be just an increase in the supertransferred hyperfine field when Fe^{3+} ions ($3d^5$) replace Co^{2+} ions ($3d^7$).[12] The reduction for $x > 0.5$ may be related to B-site canting. For $(NiZn)Fe_2O_4$, the A-site field is constant within experimental errors up to $x = 0.8$, even though Fe^{3+} ions are replacing Ni^{2+} ions ($3d^8$).[7,21] The large number of B-site nearest neighbors (twelve) accounts partially, but not fully, for the relative insensitivity of the A-site field to the nonferric B-site concentration. For $(MnZn)Fe_2O_4$, Fe^{3+} ions are present on A sites only to about $x = 0.50$. A small increase in the A-site field, about 15 kOe, is observed; however, when the experimental errors are considered, this increase may be less, perhaps only 5 kOe. As will be shown in Sec. IV B a small increase in the number of Fe^{3+} ions on B sites does occur with increasing x. However, the other ions on B sites, Mn^{2+} ($3d^5$), are expected to make the same contribution as Fe^{3+} ions to H_{sthf}. It is concluded that the A-site results for $(MnZn)Fe_2O_4$ are compatible with those for the other disordered spinels.

For both $(CoZn)Fe_2O_4$ [12] and $(NiZn)Fe_2O_4$,[7] the hyperfine field at a Fe^{3+} nucleus on a B site decreased almost linearly, as x increased from

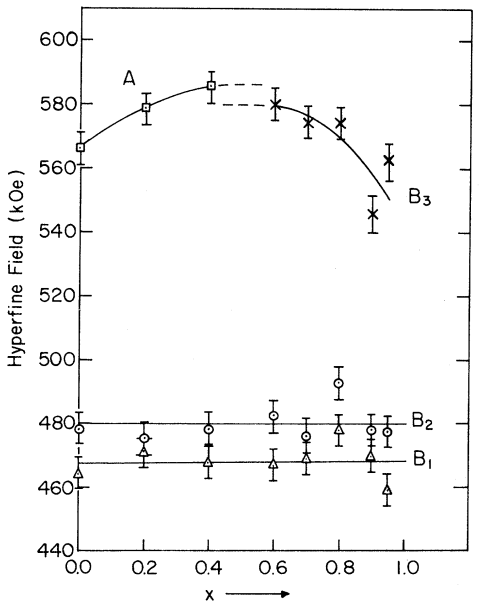

FIG. 3. Hyperfine fields in an applied field of 50 kOe plotted versus Zn concentration x.

0.0 to 1.0, by about 53 and 70 kOe, respectively, at $T = 4$ K. The decrease would appear to be due to the decrease in the transferred hyperfine field when Fe^{3+} ions on A sites are replaced by diamagnetic Zn^{2+} ions. From Fig. 3, the hyperfine field in a 50-kOe external field is essentially constant as a function of x for B_1 and B_2 sites. For $x < 0.5$, Fig. 2 shows that no measurable absorption appears for lines 2 and 5 of the Mössbauer spectra, and it follows that the spin structure is collinear with the direction of the applied field. For $x > 0.5$, lines 2 and 5 are present (Fig. 2), which implies that the B-site moments are canted at some angle with respect to the applied-field direction. The hyperfine field for zero applied field is therefore less than that at smaller x, since essentially only the component of the applied field along the ionic moments contributes to the fields plotted in Fig. 3 (strictly, these fields are vector sums). Similarly, the decrease in the B_3-site field shown in Fig. 3 is less when no field is applied. In summary then, in zero applied field the magnitudes of the B-site hyperfine fields for $(MnZn)Fe_2O_4$ are approximately constant for $0 \leq x \leq 0.5$ and decrease with increasing x for $0.5 \leq x \leq 1.0$; the decrease for $x > 0.5$ is, however, less than that observed for the other disordered spinel systems in zero applied field. It is interesting to speculate on the origins of this difference in behavior. One possibility is that B-B supertransferred hyperfine fields are more important since all, or almost all, the cations are ferric ions; it is not clear why this field should increase to compensate the decrease expected by the dilution of the A sites with zinc. However, it should be noted that the lattice parameter decreases with increasing x, the opposite to that found for $(NiZn)Fe_2O_4$.[7] Since the u parameter is almost independent of x,[16] the internuclear spacings also decrease slightly; it is conceivable that the B-B transferred hyperfine interaction then increases, and that the A-B interaction decrease is reduced in magnitude. Finally, the zero-point spin deviation contributes to the hyperfine field, and probably increases with x. Although this contribution is not important for $(NiZn)Fe_2O_4$, perhaps it is more important for $(MnZn)Fe_2O_4$.

B. Cation distributions

Information on the cation distributions was obtained from the ratio of the areas of the outermost (1 and/or 6) lines of the patterns, that is, $A(A)/[A(B_1)+A(B_2)]$ or $A(B_3)/[A(B_1)+A(B_2)]$, where A, B_1, B_2, and B_3 are the patterns with the hyperfine-field assignments of Fig. 3. Since the absorbers were relatively thin, no correction for finite thickness was made. Further, at 4.2 K there is evidence[22,23] that the recoilless fraction for ions on A and B sites are equal, and thus no error is introduced on this account. Strictly, the total area of each pattern should be used when canting occurs. However, the small absorptions for the 2 and 5 lines for $x = 0.6$ and 0.7 and the lack of resolution in the 2 and 5 lines plus possible complications in the spin configuration for $x = 0.9$ and 0.95 probably introduce as great an uncertainty in the area ratios as when only the outer lines are used. Finally, our approach also has the advantage of simplicity.

For the end member, $x = 0$, the sample formula was found to be $(Mn_{0.84}Fe_{0.16})[Fe_{1.84}Mn_{0.16}]O_4$, which agrees well with the earlier, and sometimes less accurate, results.[14-16] The iron concentration on A sites then decreases to 7% by $x = 0.40$ (see Table I and Fig. 4). In the neutron-diffraction experiments,[16] no iron was detected on A sites for $x = 0.40$; the discrepancy may be a measure of the experimental error, since small peaks are difficult to differentiate from fluctuations in background. However, Fig. 2 for $x = 0.40$ clearly shows that some Fe^{3+} ions certainly experience a larger hyperfine field.[11]

For $x > 0.5$, the relative area of the outermost absorption lines increases abruptly, as illustrated for $x = 0.8$ in Fig. 2. One possibility is that some of the Zn ions are now located on B sites, and thus displace Fe ions to A sites. However, this situation is improbable since it is contrary to experimental results for both (MnZn) and other ferrites, including $ZnFe_2O_4$. The possibility that the Mn occupancy of B sites is enhanced is even more remote. Instead, it is Fe^{3+} ions on B sites with reversed moments, the B_3 configuration, that must now be the origin of the pattern with the large hyperfine field. Of course, for $x = 0.6$, a small contribution from Fe^{3+} ions on A sites may still be present; two possible extrapolations of the data for the area ratio $A(A)/\sum A(B_n)$ are in-

TABLE I. Cation distributions for $Mn_{1-x}Zn_xFe_2O_4$ ($H = 50$ kOe).

Zn content x	Ionic formula (experiment)
0.00	$(Mn_{0.84}Fe_{0.16})[Fe_{1.84}Mn_{0.16}]O_4$
0.20	$(Zn_{0.20}Mn_{0.68}Fe_{0.12})[Fe_{1.88}Mn_{0.12}]O_4$
0.40	$(Zn_{0.40}Mn_{0.53}Fe_{0.07})[Fe_{1.93}Mn_{0.07}]O_4$
0.60	$(Zn_{0.60}Mn_{0.40})[\underline{Fe}_{0.17}Fe_{1.83}]O_4$
0.70	$(Zn_{0.70}Mn_{0.30})[\underline{Fe}_{0.33}Fe_{1.67}]O_4$
0.80	$(Zn_{0.80}Mn_{0.20})[\underline{Fe}_{0.46}Fe_{1.54}]O_4$
0.90	$(Zn_{0.90}Mn_{0.10})[\underline{Fe}_{0.68}Fe_{1.35}]O_4$
0.95	$(Zn_{0.95}Mn_{0.05})[\underline{Fe}_{0.46}Fe_{1.54}]O_4$

dicated as dashed lines in Fig. 4. However, the primary source of the outer pattern must be the B_3 configuration. The ionic formulas for the samples with $x > 0.5$ are also given in Table I, in which Fe represents the iron ions with reversed spins.

The presence of a B_3 configuration implies a localized breakdown in the antiferromagnetic A-B interaction. This is most likely when a B-site Fe^{3+} ion has all six A-site nearest neighbors occupied by diamagnetic Zn ions, an event that occurs with the probability $P(6, x) = \binom{6}{6} x^6$. To carry this idea further, the relative probability, $P(6, x)/\sum_{n<6} P(n, x)$, where $P(n, x) = \binom{6}{n} x^n (1-x)^{6-n}$, is drawn as a full curve in Fig. 4; there is respectable agreement with the data for the area ratios, at least for $0.6 \leq x \leq 0.8$. For $x = 0.6$, note that if a subtraction is made for some Fe^{3+} on A sites, given for example by the dashed lines in Fig. 4, the agreement is improved. For $x = 0.90$ and 0.95, the agreement with the proposed model becomes progressively worse. However, these samples are peculiar anyway, in that they have been reported to be antiferromagnets in zero applied field[17,18]; they will be discussed in greater detail in Sec. IV E.

Neither the A-B superexchange interaction nor the A-to-B supertransferred hyperfine interaction is likely to be zero for an Fe^{3+} B-site ion with six Zn A-site nearest neighbors, since Mn^{2+} ions on next-nearest-neighbor A sites are almost certain to enter the picture. The effects that may be anticipated are (a) a distribution in canting angles from the first interaction, to be discussed more fully in Sec. IV D, and (b) a distribution in hyperfine fields from the second interaction. A distribution in hyperfine fields would be observed either by the need to introduce one or more additional Mössbauer patterns, as for $(NiZn)Fe_2O_4$,[13] or by an increase in the linewidth of the B_3 pattern. This latter effect is indeed observed for $(MnZn)Fe_2O_4$. Specifically, at 50 kOe the average A-site linewidth ($0.0 \leq x \leq 0.4$) is 0.48 mm/sec, whereas the B_3-site linewidth starts at 0.56 mm/sec for $x = 0.60$, and then progressively increases further to 0.75 for $x = 0.70$ and to 0.83 for $x = 0.80$.

It would be desirable to extend the analysis for the B_3 sublattice to B-site Fe^{3+} ions with less than six Zn A-site nearest neighbors. For $x = 0.6$ and $x = 0.7$, there is a significant probability for four ionic configurations, viz., 5 Zn 1 Mn, 4 Zn 2 Mn, 3 Zn 3 Mn, and 2 Zn 4 Mn, whereas for $x = 0.8$, only the first three configurations are likely. However, only two additional patterns, B_1 and B_2, were required to fit the data. This lack of resolution in the spectra, which is typical for spinels at $T = 4.2$ K, inhibits the development of any quantitative analysis. It may be worthwhile to collect Mössbauer spectra at temperatures somewhat higher than 4.2 K in the hope that sufficient structure will appear in the absorption lines to permit identification of the different patterns as well as a determination of the relative line areas.

Finally, if samples were made with iron enriched in the isotope Fe^{57}, the lines of the Mössbauer spectra would possess larger relative absorptions. It may then be possible to decipher finer details in the spectra. The additional information obtained may lead to the development of a more refined model, possibly along the lines of those considered by Nowick[24] and Rosencwaig.[25]

C. Isomer shifts

The isomer shift S_{iso} for Fe^{3+} ions in different site configurations is essentially independent of zinc concentration. On the average, the values found at 50 kOe with respect to Cu were $S_{iso}(A) = 0.40$, $S_{iso}(B_1) = 0.46$, $S_{iso}(B_2) = 0.54$, and $S_{iso}(B_3)$

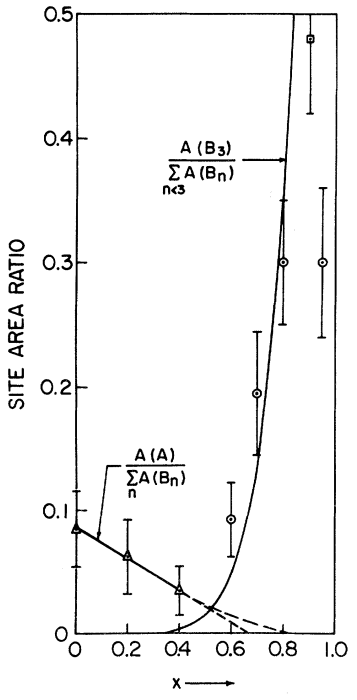

FIG. 4. Area of the outer spectral lines for Fe^{3+} ions in A or in B_3 sites compared with that in $B_1 + B_2$ normal ferrimagnetic configurations. The data was obtained for applied fields equal to 50 kOe except for $x = 0.90$, where $H = 90$ kOe. The full curve to the left is drawn through the data points for clarity; two possible extrapolations are shown by the dashed curves. The full curve to the right is the relative probability that a B-site ion has six Zn ions on nearest-neighbor sites.

= 0.45 mm/sec. Unfortunately, the experimental errors in the isomer shifts are comparable to the differences between the isomer shifts for different Fe^{3+} configurations. Although no great weight can therefore be placed on variations in the isomer shifts, it is of some interest to consider the results and their possible implications.

In the range where iron occupies A sites, $x < 0.4$, the data yield $S_{iso}(B_1) - S_{iso}(A) = 0.06$ and $S_{iso}(B_2) - S_{iso}(A) = 0.14$ mm/sec. The average, 0.10 mm/sec, is close to, but slightly less than, that observed for the differential octahedral-tetrahedral isomer shifts of other spinels. Variations in S_{iso} are expected to be due to the difference in the $Fe^{3+}-O^{2-}$ internuclear separation. This distance is smaller, and hence the covalency is larger, at the A sites than at the B sites. In addition, the difference in the two distances is slightly less for $MnFe_2O_4$ than, for example, for $NiFe_2O_4$.

Now the data show that $S_{iso}(B_3)$ is larger than $S_{iso}(A)$, so that $S_{iso}(B_1) - S_{iso}(B_3) = 0.01$. However, it is interesting that $S_{iso}(B_2)$ is consistently slightly larger than $S_{iso}(B_1)$, and on the average by 0.08 mm/sec. Although it would seem unlikely that the Fe^{3+}-O^{2-} distance could be different for B_1 and B_2 sites, it is a point that might be worthy of further investigation.

D. Magnetic structure

A canted, rather than a collinear magnetic structure, is inferred if the 2-5 lines appear in the Mössbauer spectra taken in a sufficiently large external magnetic field. For the geometry used here, the average angle θ between the directions of the applied field and the hyperfine field at a particular site is given by

$$\theta = \arcsin\left(\frac{\frac{3}{2}(A_{2,5}/A_{1,6})}{1+\frac{3}{4}(A_{2,5}/A_{1,6})}\right)^{1/2},$$

where $A_{2,5}$ and $A_{1,6}$ are the areas of lines 2 and 5 and lines 1 and 6, respectively. Because the trigonometric function enters the equation quadratically, small canting angles, say less than 10°, lead to very small, and thus barely detectable, areas $A_{2,5}$ for lines 2 and 5. For $x < 0.5$, no measurable absorptions for lines 2 and 5 were observed, and thus it is concluded that, within the experimental errors, the magnetic structure is collinear in this compositional range.

For $x > 0.5$, $A_{2,5} \neq 0$; the values of θ found (a) for the sum of the B_1 and B_2 patterns and (b) for the B_3 pattern are listed in Table II. The B_1 and B_2 patterns have been summed because the resolution is insufficient to permit reliable computations for the individual patterns.

Actually, a distribution in canting angles may be expected from the myriad of nearest- and next-nearest-neighbor configurations, particularly for the B_3 sites. However, it is practical to give only an average value for θ. Even so, because it is difficult to determine area ratios accurately from unresolved Mössbauer spectra when the line intensities are small, the errors in θ are large, especially for the B_3 sites. Nevertheless, several qualitative conclusions may be drawn from the data. The discussion in this section will be restricted to $0.60 \leq x \leq 0.80$; Sec. IV E will consider the structure for $x > 0.8$.

For $x = 0.6$ at $H = 50$ kOe, the 2-5 lines for the $B_1 + B_2$ pattern have small but nonzero intensities. The 2-5 lines for B_3 sites do appear to be present, but lie within the counting fluctuations of the background. There seemed little point in analyzing the spectrum at $H = 90$ kOe.

When x is increased to 0.7, a significant increase in canting at the $(B_1 + B_2)$ sites occurs at 50 kOe. When a field of 90 kOe is applied, the canting angle is reduced, in keeping with similar observations on $(NiZn)Fe_2O_4$.[13] The decrease of θ with field is a measure of the relative strengths of the A-B and B-B interactions compared to the torque exerted by the applied field.

The 2-5 line intensities for the B_3 sites at 50 and 90 kOe with $x = 0.7$ appear to be nonzero, but again are of the same order as the experimental uncertainties. For this reason a Mössbauer spectrum was obtained at 25 kOe. Although the resolution was poorer, B_3 2-5 lines of greater magnitude are certainly present.

Another interesting and important feature for $x = 0.7$ emerges, namely, that the occupancy of B_3 sites turns out to be field dependent. It is found that the number of Fe ions with reversed spins per formula unit is $\underline{Fe}_{0.46}$ at $H = 25$, $\underline{Fe}_{0.33}$ at $H = 50$, and $\underline{Fe}_{0.17}$ at $H = 90$ kOe. It would appear that the B_3 sublattice is incipiently unstable, and that magnetic fields of a few tens of kilooersteds

TABLE II. Average canting angle in $Mn_{1-x}Zn_xFe_2O_4$. Angles for $B_1 + B_2$ measured with respect to direction of applied magnetic field, and angles for B_3 measured with respect to the negative direction of the applied magnetic field.

	$H = 50$ kOe		$H = 90$ kOe	
x	B_3 (±50%)	B_1+B_2 (±20%)	B_3 (±50%)	B_1+B_2 (±10%)
0.60	< 12°	16°	...	...
0.70	< 12°	30°	< 10°	18°
0.80	40°	43°	13°	41°
0.90	32°	49°	15°	52°
0.95	29°	25°	...	...

are able to reinvert some of the reversed atomic moments, so that they lie along the usual B-sublattice direction, viz., that for B_1 and B_2 sites.

When $x = 0.8$, θ at 50 kOe increases further. The increase in canting with Zn content is to be expected with the reduction in the total strength of the A-B interaction, and is in accord with observations on the similar system, $(NiZn)Fe_2O_4$.[7,13] The magnetic structure for $x = 0.8$ seems to be relatively stable, at least at 4.2 K, since the canting angle and the B_3 site occupancy are essentially unchanged when the applied field goes from 50 to 90 kOe. However, the canting angle for the B_3 site does apparently decrease with an increase in the applied field.

E. $x = 0.90$ and 0.95

In view of the neutron-diffraction reports that the sample with $x = 0.87$ is antiferromagnetic ($H = 0$),[17] and that the samples with $0.82 \leq x \leq 0.87$ are ferrimagnetic with coexisting short-range antiferromagnetism,[18] the Mössbauer spectra for $x = 0.90$ and 0.95 are of special interest. The spectra in zero field have much the same appearance as for the samples with smaller x. Although there are only six absorption lines, there is a lack of symmetry in the corresponding pairs of lines. Also, the linewidths are wider than would be expected for a simple uniaxial antiferromagnet. Of course, a simple antiferromagnetic structure has not been claimed; although the matter is not settled, the structure seems to consist of four sublattices. It is possible that line broadening may result from variations in the electric quadrupole interactions, since the angle between the hyperfine field and the principal axis of the electric-field-gradient tensor may be different for each sublattice.

It is therefore particularly important to examine the Mössbauer spectrum in an applied field. The spectra for $x = 0.90$ in fields of 50 and 90 kOe are shown in Fig. 5. Because of the better resolution, the spectrum at 90 kOe will be considered in greatest detail. The spectrum is rather similar to those with $0.6 \leq x \leq 0.8$, and can be fitted adequately with only three patterns. A distinct and large increase in the linewidth to 1.43 mm/sec does occur for the pattern with the largest hyperfine splitting (the B_3 sites). For the two other patterns (B_1 and B_2), both have a smaller linewidth increase to about 0.72 mm/sec. However, an even larger increase in the B_1 and B_2 linewidths would have been expected for a four-sublattice antiferromagnet. The observed linewidths are probably compatible with the increase in the hyperfine field distribution expected for a ferrimagnet with higher Zn concentration.

The area ratios for the two samples, $A(B_3)/[A(B_1)+A(B_2)]$, do fall well below the curve for the relative probability for six Zn nearest A neighbors in Fig. 4. However, the same behavior was observed for $(NiZn)Fe_2O_4$,[13] and it was suggested that saturation effects might be limiting the number of reversed B spins.

Clearly, the system is canted. If the system were a four-sublattice antiferromagnet, a 2-5 line would also appear in the spectrum. Indeed, if two of the sublattices were perpendicular to the applied field direction, it seems likely that the areas of the 2-5 lines would be much bigger than those observed. Actually, the degree of canting is consistent with that observed at lower zinc concentrations, for example for $x = 0.80$ (see Table II). Therefore it follows that the non-zero field spectra are consistent with those expected for a canted ferrimagnet with more than one B-site spin configuration, including reversed atomic moments at some sites.

The question, then, is how to reconcile the antiferromagnetic structure found by neturon diffraction with the ferrimagnetic structure inferred from the Mössbauer spectra. Since the lattice parameter for $x = 0.87$ determined by Fayek *et al.*[17] agrees very well with those for our samples (see Fig. 1), it seems unlikely that uncertainties in composition could be the explanation. Further, there seems to be no reason to question the interpretation of the neutron-diffraction spectra, including the choice of magnetic cell. The prime difference in the experimental conditions is the presence of a large external magnetic field. Per-

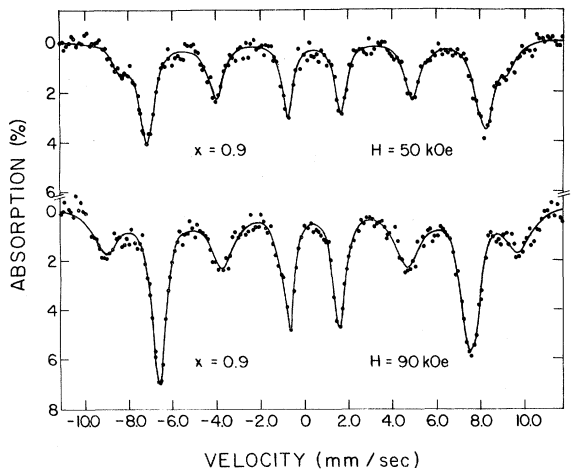

FIG. 5. Mössbauer spectra for $x = 0.90$ in external magnetic fields of 50 and 90 kOe. The full curve is the sum of three six-line patterns, B_1, B_2, and B_3.

haps the antiferromagnetic structure in zero field is just barely stable, and switching on a magnetic field can tip the scales to make a ferrimagnetic structure the stable one. A hint that this idea may be correct comes from the observation that on going from 50 to 90 kOe some of the variables are less stable than for $x = 0.80$, that is, the canting angle for $B_1 + B_2$ sites *increases* slightly (see Table II), and the B_3-site linewidth increases significantly. Another point is that according to Fayek *et al.*[17] the Néel temperature is only 11K for $x = 0.87$, and therefore the magnetic field interaction will be comparable to the superexchange interactions. It would be of interest to have the neutron-diffraction studies extended to include the presence of a large external magnetic field.

V. CONCLUSIONS

The family of spinels $Mn_{1-x}Zn_xFe_2O_4$ has a cation distribution which permits definitive information on the magnetic structure to be obtained from Mössbauer spectra collected in large applied magnetic fields. Indeed, in this respect, the compounds are unique amongst the magnetically disordered ferrite systems studied to data. For low zinc concentrations, a small number of ferric ions, up to a maximum of 8% for $x = 0$, occupy tetrahedral sites. Above $x = 0.5$, at least 99% of the ferric ions are located at octahedral sites. The magnetic structure is collinear for $x < 0.5$ within the experimental errors. Above $x = 0.5$, the Fe^{3+} ions are canted with respect to the applied field direction, the degree depending on the number of Zn ions on the nearest-neighbor A sites. When all six neighbors are diamagnetic Zn^{2+} ions, the spin of the B-site Fe ion is reversed, and exhibits a large hyperfine field. The degree of canting increases with increase in zinc content, and is usually reduced in larger applied fields. However, the sample with $x = 0.80$ has a relatively stable magnetic structure. At $x = 0.90$ and 0.95, the high-field data are consistent with a ferrimagnetic structure. It is possible that the antiferromagnetic structure implied by neutron diffraction in zero fields is unstable when a large magnetic field is applied. The hyperfine fields show only a small change with x, which is somewhat surprising in view of the decrease expected in the supertransferred hyperfine field when zinc replaces manganese on the A sites. The isomer shifts are consistent with those found in other magnetic spinel systems.

ACKNOWLEDGMENTS

We are indebted to A. Vas (Monash) for making the samples and to N. Hall (Manitoba) for the powder-diffractometer measurements. One of us (A. H. M.) would like to thank R. Street for making a sabbatical leave at Monash possible, useful, and enjoyable.

[1] C. Guillaud and H. Creveaux, C. R. Acad. Sci. (Paris) 230, 1458 (1950).
[2] B. J. Evans, in *Proceedings of the Fourth Symposium on Mössbauer Effect Methodology*, edited by I. J. Gruverman (Plenum, New York, 1968), and references therein.
[3] E. Wieser, V. A. Povitskii, E. F. Makarov, and K. Kleinstück, Phys. Status Solidi 25, 607 (1968).
[4] V. F. Belov, N. S. Ovanesyan, V. A. Trukhtanov, M. N. Shipko, E. V. Korneev, V. V. Korovushkin, and L. N. Korablin, Zh. Eksp. Teor. Fiz. 59, 1484 (1970) [Sov. Phys.—JETP 32, 810 (1971)].
[5] V. I. Goldanski, V. F. Belov, M. N. Devisheva, and V. A. Trukhtanov, Zh. Eksp. Teor. Fiz. 49, 1681 (1965) [Sov. Phys.—JETP 22, 1149 (1966)].
[6] J. M. Daniels and A. Rosencwaig, Can. J. Phys. 48, 381 (1970).
[7] L. K. Leung, B. J. Evans, and A. H. Morrish, Phys. Rev. B 8, 29 (1973).
[8] G. A. Petit, Solid State Commun. 13, 1611 (1973).
[9] L. Cser, I. Dézsi, I. Gladkih, L. Keszthelyi, D. Kulgawczuk, N. A. Eissa, and E. Sterk, Phys. Status Solidi 27, 131 (1968).
[10] U. König, Y. Gros, and G. Chol, Phys. Status Solidi 33, 811 (1969).
[11] Sh. Sh. Bashkirov, A. B. Liberman, and V. I. Sinyavskii, Fiz. Tverd. Tela 14, 3264 (1972) [Sov. Phys.-Solid State 14, 2776 (1973)].
[12] G. A. Petit and D. W. Forester, Phys. Rev. B 4, 3912 (1971).
[13] P. E. Clark and A. H. Morrish, Phys. Status Solidi A 19, 687 (1973).
[14] J. H. Hastings and L. M. Corliss, Phys. Rev. 104, 328 (1961).
[15] G. A. Sawatzky, F. van der Woude, and A. H. Morrish, Phys. Lett. A 25, 147 (1967).
[16] U. König and G. Chol, J. Appl. Crystallogr. 1, 124 (1968).
[17] M. K. Fayek, J. Leciejewicz, A. Murasik, and I. I. Yamzin, Phys. Status Solidi 37, 843 (1970).
[18] A. Loshmanov, S. Ligenza, M. K. Fayek, and A. G. Kocharov, Phys. Status Solidi A 7, K71 (1971).
[19] U. König, E. F. Bertaut, Y. Gros, M. Mitrikov, and G. Chol, Solid State Commun. 8, 759 (1970).
[20] B. Boucher, R. Buhl, and M. Perrin, Phys. Status Solidi 40, 171 (1970).
[21] H. Abe, M. Matsuura, H. Yasuoka, A. Hirai, T. Hashi, and T. Fukuyama, J. Phys. Soc. Jpn. 18, 140 (1963).
[22] G. A. Sawatzky, F. van der Woude, and A. H. Morrish, Phys. Rev. 187, 747 (1969).
[23] B. J. Evans and S. S. Hafner, J. Phys. Chem. Solids 29, 1573 (1968).
[24] I. Nowick, J. Appl. Phys. 40, 872 (1969).
[25] A. Rosencwaig, Can. J. Phys. 48, 2857 (1970); Can. J. Phys. 48, 2868 (1970).